
Single Pixel Imaging using Compressive Sensing and Spatial Light Modulator

Mohammad Roueinfar^{a*}, Mahdi Salmanian^b, Ali Aghakasiri^c, Abbas Bashiri^d, Saeed Babanezhad^e

^{a,b,d,e}Department of Electrical Engineering, IHU, Tehran, Iran

^cPh.D. Student of Communication, Department of Electrical Engineering, Sharif University, Tehran, Iran

Received 18 March 2021; revised 13 May 2021; Accepted 13 August 2021

Abstract

Conventional cameras based on an array of pixels (CCD or CMOS) are commonly used to capture a target image at a certain distance. In this type of camera, all pixels are used to create the image. For CCD-based cameras at other wavelengths, including infrared and terahertz, having all the pixels increases the cost of the camera. The aim of this study is to design and build an imaging setup using a single pixel method to reduce the cost of the camera and to reconstruct the target image using less data. We verify this method for visible band due to availability of visible light equipment that can be generalized this method to other wavelengths. We use a spatial light modulator (SLM) produces two-level optical masks with random distribution with 20 x 20 pixels and a size of 10 x 10 cm and illuminates the target at a repetition rate 1 Hz. The reflection of each mask from the target captured by a CCD camera and then we average all pixels of the CCD to equate it with a single-pixel detector. The target image is reconstructed using a compressive sensing algorithm. The process of reconstructing the target image is performed using a minimum number of masks. We use the two norms L1 and TV to retrieve the target image. The simulation results show TV norm is more successful in target image retrieval. Also, with increasing the number of masks, the success rate in retrieving the target image increases.

Keywords: Single Pixel Method, Mask, Spatial Light Modulator, Compressive Sensing, Measurement, Pattern

1. Introduction

The Single-pixel imaging system is a new method that enables low-cost imaging, hardware and software compression of data (Rousset, 2017). The applications of single-pixel imaging include biomedical imaging (Jacques, 2013), microscopic fluorescence imaging (Studer et al, 2012), tomography (Huynh et al, 2019), non-destructive testing and classification of explosive materials (Majumder et al, 2020), visible telescope-NIR (Yu at al, 2014), and compressive radar imaging

* Corresponding author Tel: +98-9127579375.

Email address: mrooein@hotmail.com .

(Baraniuk and Steeghs, 2007). At first glance, having a single-pixel imaging system may not make much sense compared to today's multi-million-pixel cameras. However, this type of imaging systems has advantages compared to cameras based on CCD or CMOS architecture. The Single-pixel detectors are generally so efficient that they are a suitable option for detection when the intensity of incoming light is very low (Hadfield, 2009).

Considering single pixel detectors from a hardware point of view, since only one pixel is used to collect data, it will definitely requires less storage memory compared to array detectors (Ma, 2009). Another importance of this type of camera is the spectral imaging area, so that the cost of CCD or CMOS is very high in near, middle and far infrared and terahertz areas (Hornett et al., 2016), while the single-pixel detectors are less expensive.

For the first time, the concept of light field modulation and light output collection on a single-pixel detector was reported in 1982. Using the piezoelectric-elasto-optical effect of an optical crystal, the incoming light has been modulated so that the light output was proportional to the Fourier transform of the object (Ben-Yosef and Sirat, 1982). In 2005 by Sen et al, a photography (imaging) method is proposed that showed the basic idea of photographing objects using only a single-pixel optical detector compared to array-based and SLR cameras. After proving the optical modulation process and one year after the idea of Sen et al, the first image was taken by a single-pixel detector at Rice University (Candès et al, 2006; Donoho, 2006; Wakin et al, 2006; Candès and Tao, 2006). Then, in 2006, Donoho implemented the compressive sensing (CS) processing algorithm for the first time (Donoho, 2006), so that Takhar et al used this idea to reconstruct the image of different targets using random patterns. In this method, the target image is reconstructed by a single-pixel detector when the number of measurements is less than the total number of pixels in the image (Takhar et al, 2006). Since the imaging platform consists of a single-pixel detector, the CS algorithm is a practical and cost-effective idea, it was also used in other areas of the electromagnetic spectrum. In 2008, Chan designed and built the first single-pixel imaging system in the terahertz spectral region (Chan et al, 2008). Howland in 2011, designed a laser radar camera capable of making 3D images using a laser light source and a single-pixel detector (Howland et al, 2011). In 2015, Wen-Kai retrieved images of targets at a distance of 2 km using a CS algorithm, a single-pixel detector and a telescope system (Wen et al, 2015). Gibson in 2017, photographed a methane gas leak using a single-pixel camera in real time (Gibson et al, 2017) and Radwell in 2019, designed a Lidar using a single-pixel detector and spatial light modulator (SLM) (Radwell et al, 2019). Depending on the structure and modulation type of the incoming light signal, the spatial light modulators are divided into several general categories, including digital micro-mirror device (DMD), liquid crystal device (LCD), liquid crystal on silicon (LCoS), metamaterials and mechanical masks. Each of the mentioned SLMs has certain considerations which will be mentioned in the following.

DMDs are an array of digital micro-mirrors based on the software patterns with light and dark pixels sent to the DMD and modulate the input light in the range of about 400-800 nm (Lee, 2008). In the structure of LCD-based modulators, which consist of an array of liquid microcrystals, each pixel contains a liquid crystal sandwiched between two electrodes, two glasses and two polarizers with parallel polarization (holoeye, 2012). The spatial light modulation by LCoS modulators is similar to LCD because it has a liquid crystal-based structure, except that it modulates light in reflection mode. In the structure of metamaterial modulators, each pixel consists of artificial electromagnetic materials with electrical permittivity $\epsilon(\omega)$ and magnetic permeability $\mu(\omega)$ determined by the geometry of the components of the material. The implementation of a software pattern on the incoming light is such that applying the pattern with light and dark pixels electronically to the metamaterial changes the absorption coefficient of the metamaterial (Watts et al, 2016). The mechanical masks are another type of optical spatial modulator, except that the software pattern is implemented on a physical substrate such as plastic (Hayasaki and Sato, 2020), metal such as copper, steel, or even gold (He et al, 2020).

In this paper, we propose a single pixel imaging method for reflective mode in visible band. We use a white light source, in reflection mode, using a LCD as SLM performed for a distance of 3 meters. The aim of this study is to design and build an imaging setup using a single pixel method to reduce the

cost of the camera and to reconstruct the target image using less data.

2. Material and Method

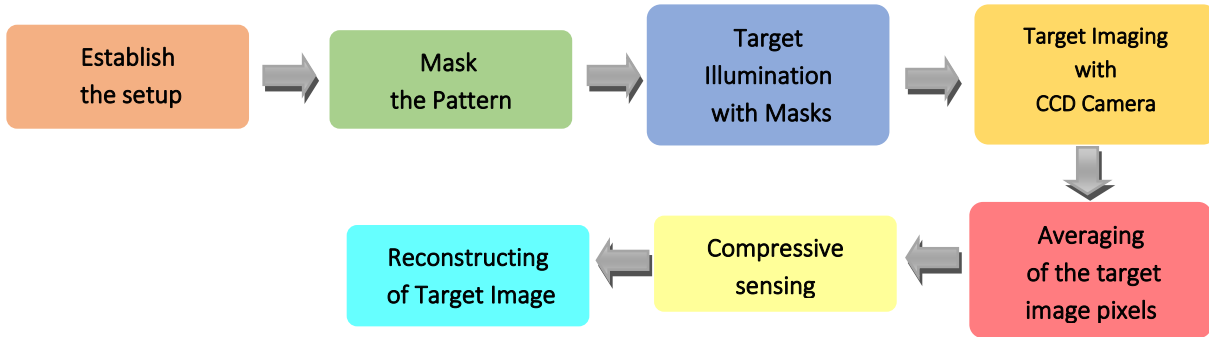


Figure 1. Steps of proposed imaging method

2.1. Establish the Setup

The single-pixel imaging arrangement in the visible area is shown in Figure 2. The two-level patterns with random distributions sent by the computer to a CP-X2510 LCD-model projector (SLM) with a resolution of 786×1024 pixels and are displayed by the projector at a repetition rate of 1 Hz along the target. Of course, according to the technical specifications of the projector, the repetition rate can be increased up to 60 Hz. In front of the projector there is a “Samyang 500 mm f/6.3” model imaging lens with a focal length of 500 mm and a field of view of 5 degrees to prevent the masks from diverging too much during propagations.



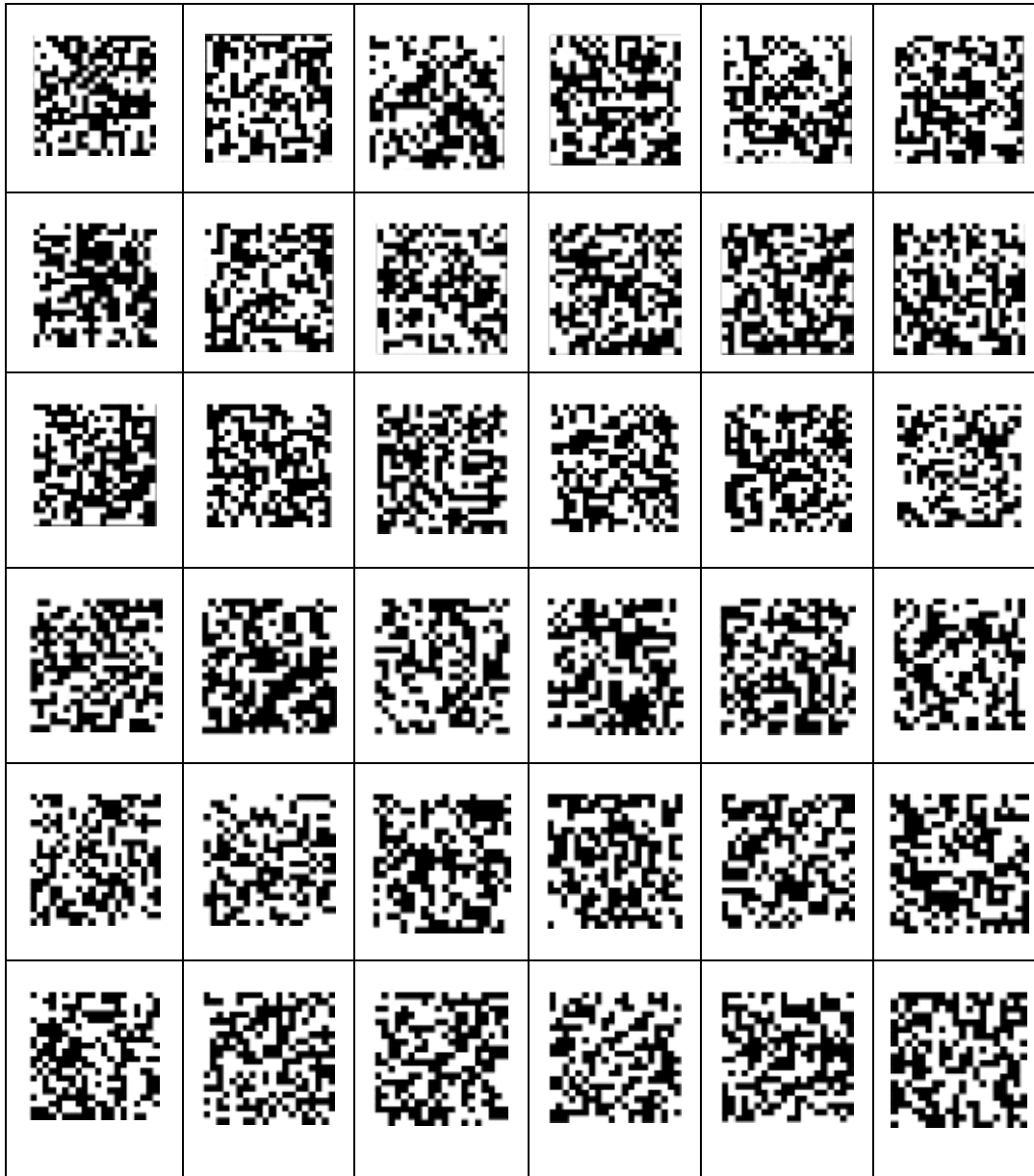
Figure 2. The single-pixel imaging arrangement in the visible area

The beam modulated by each mask, radiates on a target at a distance of 3 meters, and after the beam is reflected, the target image is recorded by the "SDZ-370" camera with a focal length of 129.5 mm

and a horizontal field of view of 55.5 degrees.

2.2. Mask the Pattern

In the next step, we produce the masks in the form of 20 by 20 matrices using MATLAB software. According to Figure 3, white squares mean light rays and black squares mean no light rays. These masks are produced randomly and with a statistical distribution of Bernoulli type. Figure 3 shows all 60 two-level masks.



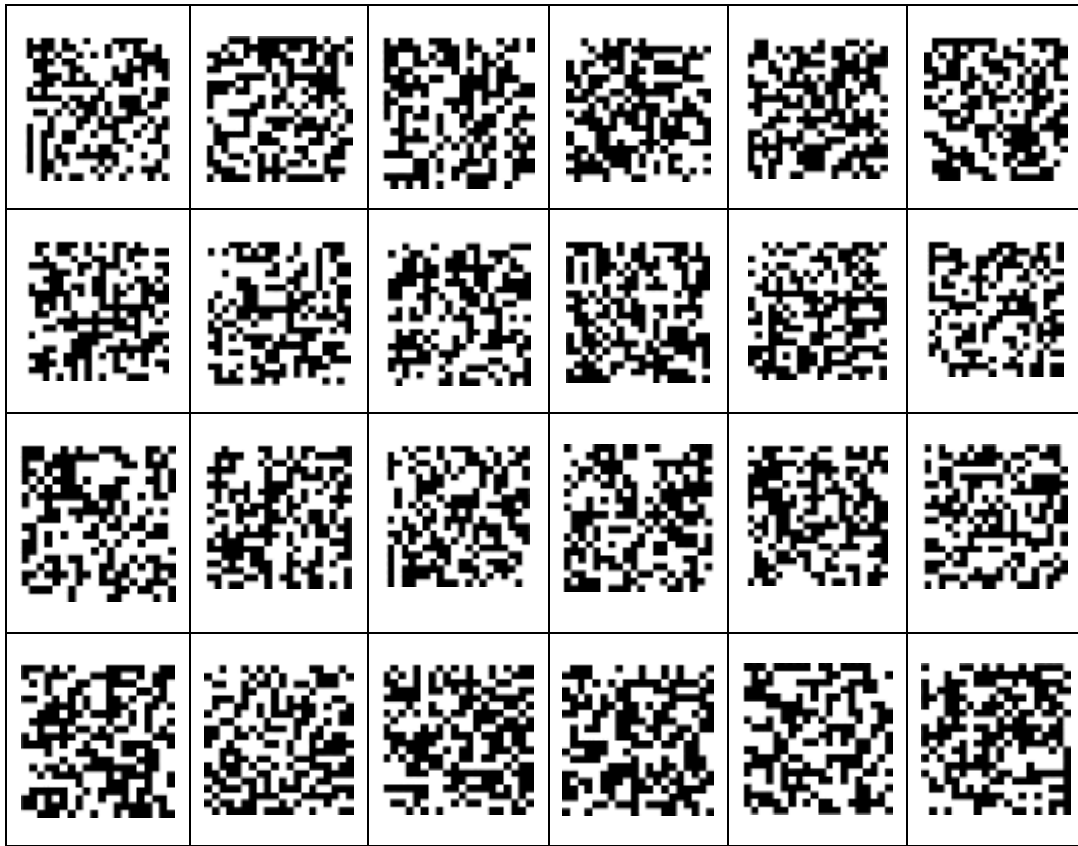


Figure 3. The two-level mask patterns with random distribution.

2.3. Target Illumination with Masks

The masks are modulated by the light beam of projector and modulated light illuminates through the lens on the target and the target is a "F" letter.

2.4. Target Imaging with CCD Camera

In the following, using a CCD camera we capture the image of target illuminated by a modulated light. Figure 4 shows the target image illuminated by modulated light for a mask.



Figure 4. The target image illuminated by modulated light for a mask.

2.5. Averaging of the Target Image Pixels

Then, by averaging all the pixels generated in the target image recorded by the camera, for each mask, a unique data is obtained that is equal to the average of pixels of each image per mask. The purpose of averaging at this stage is to equate a single-pixel detector in the visible band. Although it is not difficult to provide CCD in the visible band, our goal is to prove the compressive sensing method for single-pixel imaging in other bands, which for simplicity, we started with the visible band.

2.6. Compressive Sensing

In following, the image generated by camera and read in MATLAB and averaged and convert to a single data just like when received with a single pixel detector. Therefore, to recover the image with N pixels, N different measurements are required. To perform these measurements, masks are needed to pass waves in some pixels and not pass waves in other pixels. If the number of measurements is equal to the number of pixels, then CS algorithms are not used. If the number of measurements is less than the number of pixels, it is required to use CS algorithms. In CS, the problem model is as the following relationship:

$$\mathbf{y}_{m \times 1} = \mathbf{A}_{m \times n} \mathbf{x}_{n \times 1} \quad (1)$$

In this relationship y is the measurement vector and m are the number of measurements, A is the sampling matrix and x is the image vector. The aim is to find the sparsest answer to this equation. To solve this equation, we could minimize L1 norm or TV norm (Donoho, 2006).

$$\text{minimize } \|\mathbf{x}\|_1 \quad \text{s.t. } \mathbf{y}_{m \times 1} = \mathbf{A}_{m \times n} \mathbf{x}_{n \times 1} \quad (2)$$

$$\text{minimize } \|\mathbf{x}\|_{TV} \quad \text{s.t. } \mathbf{y}_{m \times 1} = \mathbf{A}_{m \times n} \mathbf{x}_{n \times 1} \quad (3)$$

Total variation is the sum of vertical and horizontal variation of each row of an image. We have developed an active illumination single-pixel imaging system. Using the video projector, we illuminate the random binary measurement matrix on the object. The total number of measurements is $M = 60$. The image size is $N=400$. So, the sampling rate is $M/N = 15\%$. In the next step, for generating the y vector, we need to use received images. To average the image pixels, the following equation is used

$$\mathbf{y}(s) = \frac{1}{N} \sum_i \sum_j b_s(i, j) \quad (4)$$

In this equation \mathbf{b}_s is the pixels of received image. To generate the measurement vector, we used the equation above.

2.7. Reconstructing of Target Image

In this step, by solving the (2) and (3), we extract the image vector x using compressive sensing algorithm and two norms L1 and TV. We use two solvers to solve (2) and (3) using SPGL1 (E. van den Berg et al, 2008) and NESTA (Becker et al, 2011) solvers.

3. Results and Discussion

Here we use the setup shown Figure2. Using the masks produced in section 2-2 and Figure 3, the

light is modulated by the projector and projected onto the target, which is the letter "F". The target image, illuminated by modulated light, captured by a CCD camera. The images taken from the target, equal to the number of masks, are averaged. So, we have a measurement vector y . In the first test, we use 60 masks. So, the measurement vector of y is $60 * 1$. We retrieve the target image using a compressive sensing algorithm and two norms, L1 and TV. The simulation results obtained from the compressive sensing algorithm using the two norms L1 and TV are shown in the Figure 5.

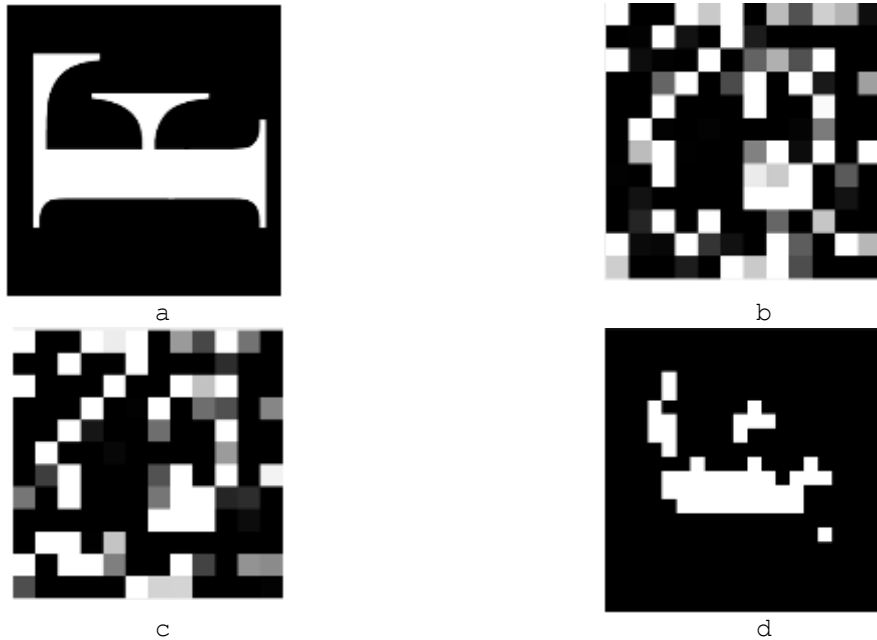


Figure 5. The results of image reconstruction using CS algorithm and 60 Masks. a) Original Image. b) Reconstructed Image by L1 norm (SPGL1 solver) c) Reconstructed Image by L1 norm (NESTA solver) d) Reconstructed Image by TV norm (NESTA solver)

As shown in the figure above, due to the small number of masks compared to the total number of pixels, the reconstructed image in NESTA mode and TV norm (Fig.5-d) is more acceptable. In the second test, we recover the target for different numbers of masks. Considering the number of masks as 40, 50 and 60 masks, the results of second test are shown in Figure 6.

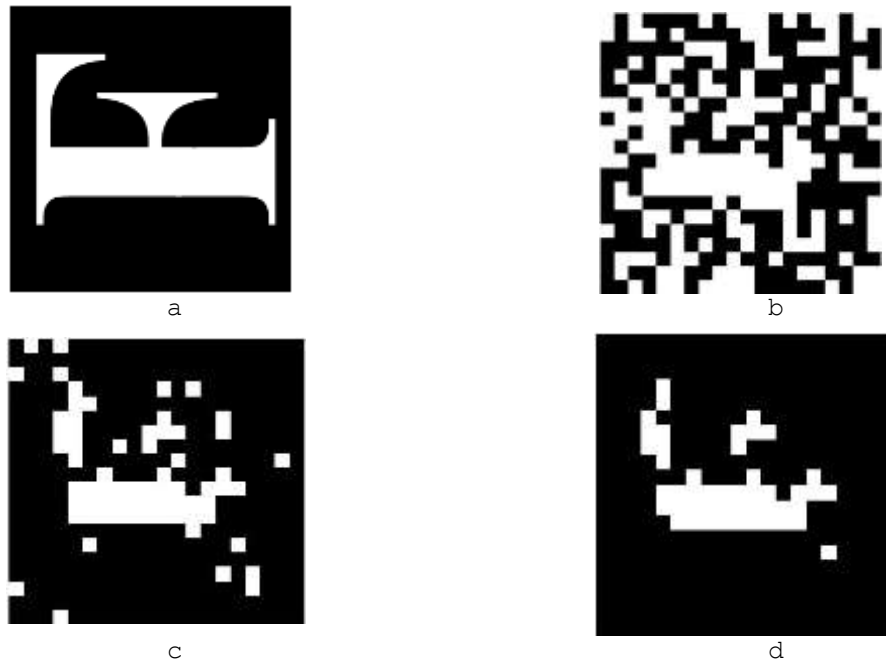


Figure 6. The results of image reconstruction using CS algorithm using a) Original Image. b) 40 Masks. c) 50 Masks. d) 60 Masks

As shown in the figure above, due to the small number of masks compared to the total number of pixels, the reconstructed image in NESTA mode is an acceptable image. According to Figure 6, the more masks, the recovered image is closer to the target image. To quantify the difference between the recovered image and the original image, we use a quantitative criterion named RMSE. As shown in Figure 7, the greater the number of masks, the RMSE is smaller, in other words, the greater the number of masks leads to the smaller the difference between the recovered image and the original image.

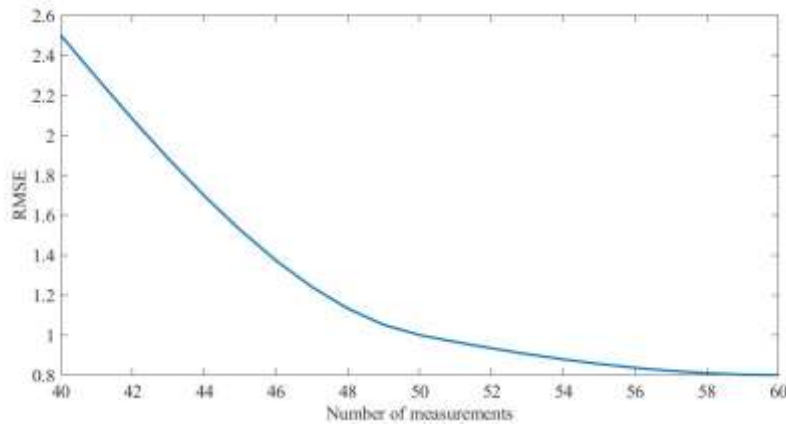


Figure 7. The RMSE of proposed imaging method

At the end, we compare our imaging method with other methods (Sun et al., 2013) use four single-pixel detectors to reconstruct a three-dimensional image, while in our imaging method only one single pixel (averaging on CCD pixels) is used for reconstruction. (Leihong et al., 2021) has recovered the

image from a laser light source, in transmission mode, using a DMD as SLM, at a distance of less than 1 meter, while in our imaging method, the process of target imaging using a white light source, in reflection mode, using a LCD as SLM performed for a distance of 3 meters. (Phillips et al., 2017) use Hadamard masks and 50 mm lenses for reconstructing the target image using a super sampling method, while in our imaging method, we use two-level masks with Bernoulli distribution, a 500 mm lens, a narrow field of view and compressive sensing method.

4. Conclusion

In this paper, a single-pixel imaging method presented in reflective mode using the spatial light modulation and compressive sensing algorithm. We used the software masks, a video projector, a lens in the visible band and 60 two-level masks with random distribution and 20×20 -pixel resolution and 1 Hz frame rate. Then the modulated light radiated on a target at a distance of 3 meters. To equate the single-pixel detector in the visible band, the pixel averaging method of the target image used and finally, the modulated image retrieved using the compressive sensing algorithm. The results showed that the use of TV norm in retrieving the target image is more successful than L1 norm.

References

- Baraniuk, R., & Steeghs, P. (2007). Compressive radar imaging. *IEEE radar conference*, 128–133.
- Ben-Yosef, N., & Sirat, G. (1982). Real-time spatial filtering utilizing the piezoelectric-elasto-optic effect. *Optica Acta: International Journal of Optics*, 29(4), 419–423.
- Becker, S., Bobin, J., & Candès, E. J. (2011). NESTA: A fast and accurate first-order method for sparse recovery. *SIAM Journal on Imaging Sciences*, 4(1), 1-39.
- Candès, E. J., Romberg, J. K., & Tao, T. (2006). Stable signal recovery from incomplete and inaccurate measurements. *Commun. Pure Appl. Math.* 59(8), 1207–1223.
- Chan, W. L., Charan, K., Takhar, D., Kelly, K. F., Baraniuk, R. G., & Mittleman, D. M. (2008). A single-pixel terahertz imaging system based on compressed sensing. *Appl. Phys. Lett.* 93(12).
- Donoho, L. (2006). Compressed sensing. *IEEE Trans. Inf. Theory* 52(4), 1289–1306.
- Gibson, G. M., Sun, B., Edgar, M. P., Phillips, D. B., Hempler, N., Maker, G. T., Malcolm, G. P. A and Padge, M. J. (2017). Real-time imaging of methane gas leaks using a single-pixel camera. *Opt. Express* 25(4), 2998–3005.
- Hadfield, R. H. (2009). Single-photon detectors for optical quantum information applications. *Nature photonics*, 3(12), 696–705.
- Hayasaki, Y., & Sato, R. (2020). Single-pixel camera with hole-array disk. *Optical Review*, 252-257.
- He, Y-H., Zhang, Ai-X., Li, M-F., Huang, Y-Y., Quan, B-G., Li, D-Z., Wu, L-A., & Chen, L-M. (2020). High-resolution sub-sampling incoherent x-ray imaging with a single-pixel detector. *APL Photonics*, 5, 056102-1:056102-7.
- Holoeye. (2012). *lc-2012-spatial-light-modulator*. Retrieved from holoeye: /holoeye.com
- Hornett, S. M., Stantchev, R. I., Vardaki, M. Z., Beckerleg, C., & Hendry, E. (2016). Subwavelength terahertz imaging of graphene photoconductivity. *Nano Lett.* 16(11), 7019–7024.
- Howland, G. A., Dixon, P. B., & Howell, J. C. (2011). Photon-counting compressive sensing laser radar for 3D imaging. *Appl. Opt.* 50(31), 5917–5920.
- Huynh, N., Lucka, F., Zhang, E. Z., Betcke, M. M., Arridge, S. R., Beard, P. C., & Cox, B. T. (2019). Single-pixel camera photoacoustic tomography. *Journal of Biomedical Optics*, 24(12). doi:10.1117/1.JBO.24.12.121907
- Jacques, S. L. (2013). Optical properties of biological tissues: a review. *Physics in Medicine and Biology*, 58(11), R37-61. doi:doi: 10.1088/0031-9155/58/11/R37.
- Lee, B. (2008). *Introduction to ± 12 Degree Orthogonal Digital Micromirror Devices (DMDs)*. Retrieved from ti: www.ti.com
- Leihong, Z., Zhixiang, B., Hualong, Y., Zhaorui, W., Kaimin, W., & Dawei, Z. (2021). Restoration

- of Single pixel imaging in atmospheric turbulence by Fourier filter and CGAN. *Applied Physics B*, 1-16.
- Ma, J. (2009). Single-pixel remote sensing. *IEEE Geoscience and Remote Sensing Letters*, 6(2), 199–203.
- Majumder, S., Gupta, S., & Dubey, S. (2020). Spectral imaging using compressive sensing-based single-pixel modality. *Electronic letters*. doi:10.1049/el.2020.0757
- Phillips, D. B., Sun, M-J., Taylor, J. M., Edgar, M. P., Barnett, S. M., Gibson, J. M., & Padgett, M. J. (2017). Adaptive foveated single-pixel imaging with dynamic super sampling. *Applied Optics*, 1-10.
- Radwell, N., Johnson, S. D., Edgar, M. P., Higham, C. F., Murray-Smith, R and Padgett, M. J. (2019). Deep learning optimized single-pixel lidar. *Appl. Phys. Lett.* 115(23).
- Rousset, F. (2017). *Single-pixel imaging : Development and applications of adaptive methods*. Lyon. Retrieved from <https://tel.archives-ouvertes.fr/tel-02067934/document>
- Sen, P., Chen, B., Garg, G., Marschner, S. R., Horowitz, M., Levoy, M., & Lensch, H. P. A. (2005). Dual Photography. *ACM Trans. Graph*, 24(3), 745–755.
- Studer, V., Bobin, J., Cahid, M., Mousavi, H. S., Candes, E., Dahan, M. (2012). Compressive fluorescence microscopy for biological and hyperspectral imaging. *Proc Natl Acad Sci U S A*, 109(26), E1679-87. doi:DOI: 10.1073/pnas.1119511109
- Sun, B., Edgarr, M. P., Bowman, R., Vitterts, L. E., Welsh, S., Bowman, A., & Padgett, M. J. (2013). 3D Computational Imaging with Single-Pixel Detectors. *Science*, 844-847.
- Takhar, D., Laska, J. N., Wakin, M. B., Duarte, M. F., Baron, D., Sarvotham, S., Kelly, K. F., & Baraniuk, R. G. (2006). A new compressive imaging camera architecture using optical-domain compression. In: *in Proc. of Computational Imaging IV at SPIE Electronic Imaging*, (pp. 43-52).
- Tao, T., Candès, E. J. (2006). Near-optimal signal recovery from random projections: Universal encoding strategies? *IEEE Trans. Inf. Theory*, 52(12), 5406–5425.
- van den Berg, E., & Friedlander, M. P. (2008). Probing the Pareto frontier for basis pursuit solutions. *SIAM J. on Scientific Computing*, 31(2), 890-912.
- Wakin, M. B., Laska, J. N., Duarte, M. F., Baron, D., Sarvotham, S., Takhar, D., Kelly, K. F., & Baraniuk, R. G. (2006). An architecture for compressive imaging. *International Conference on Image Processing*, (pp. 1273–1276).
- Watts, C. M., Nadel, C. C., Montoya, J., Krishna, S., & Padilla, W. J. (2016). Frequency-division-multiplexed single-pixel imaging with metamaterials. *Optica*, 133-138.
- Yu, W-K., Liu, X-F., Yao, X-R., Wang, C., Zhai, Y., & Zhai, G-J. (2014). Complementary compressive imaging for the telescopic system. *Scientific Reports*. doi:10.1038/srep05834